Quaternary Research 56, 275–287 (2001)
doi:10.1006/qres.2001.2240, available online at http://www.idealibrary.com on IDEAL®

Late Holocene Paleoclimatic Changes in Western Central Africa Inferred from Mineral Abundance in Dated Sediments from Lake Ossa (Southwest Cameroon)

Denis Wirrmann and Jacques Bertaux

IRD, UR 55 Paléotropique, 32 Avenue Henri Varagnat, 93143 Bondy cedex, France

E-mail: Denis.Wirrmann@bondy.ird.fr

and

Alice Kossoni

Université 1 de Yaoundé, Cameroon

Received May 9, 2000; published online June 27, 2001

Minerals derived from catchment soils were determined using FTIR spectroscopy in the well-dated core OW4 from Lake Ossa, a lowland rainforest area in Cameroon. This quantification provides a hydrologic record indicating that the magnitude of runoff events, and by inference, rainfall pattern, has varied during the Late Holocene. The comparison between minerogenic inputs and vegetation changes improves the understanding of the inferred climate dynamics. Since at least 5400 cal yr B.P., the paleomonsoon rainfall intensity decreased, as shown by a general decrease in mineral fluxes. This observation is consistent with a gradual weakening of the boreal summer insolation in tropical latitudes. However, the major vegetational change lags behind the onset of the decrease in mineral fluxes. From 2800 to ca 1000 cal yr B.P., the forest receded: the amount of rainforest taxa decreased and is replaced by pioneer trees and Poaceae, when the mineral fluxes attained their lowest values. This episode of maximum dryness is attributed to an abrupt climatic event of global significance which is superimposed onto the paleomonsoon variability. It is related to a cold event, which in turn produced a change in the lower atmospheric circulation that was characterized by a strengthening of northern trade winds, probably correlated with sea-surface temperature variations in the eastern tropical Atlantic area. © 2001 University of Washington.

Key Words: FTIR mineral quantification; detrital fluxes; Late Holocene; paleoclimatic changes; Cameroon; Western and Central Atlantic Africa.

INTRODUCTION

Previous studies have shown that environmental and climatic conditions during the Late Quaternary in the rainforest realm of Western and Central Atlantic Africa differed significantly from those now prevailing over this area (Maley 1991; Pokras and Mix, 1985; Street-Perrott and Perrott, 1993; Vincens *et al.*, 1999). In this lowland humid region, located within the domain of the permanent Atlantic monsoon, climatic fluctuations expressed themselves as changes in the hydrological balance, involving precipitation, evaporation, and runoff. While evaporation and runoff undoubtedly played a part, rainfall variation was the decisive factor in these environmental modifications. To precisely determine the timing of the rainfall fluctuations, a multiple proxy approach is necessary, owing to the specific inertia of each individual paleoenvironmental parameter. This is especially so when the study area is located in the rainforest realm, an environment which is rather insensitive to small changes in rainfall. Notable transformations of the rainforest cover will occur only beyond a certain threshold, when environmental boundary conditions are reached. That is why the timing of rainfall fluctuations can be misinterpreted if it is based solely on the vegetation changes, the dynamics of which is unknown. As most of the earlier paleoclimatic studies of continental records in this area were based mainly on vegetation evolution inferred from palynological data (Elenga *et al.*, 1996; Giresse *et al.*, 1994; Maley, 1996; Vincens *et al.*, 1998), we propose to use the mineral contents of the sediments to characterize the sedimentary dynamics, and thus the paleoenvironmental changes. Indeed, the good chronological control enables the computation of the fluxes of mineral inputs from the surrounding soils into the lake basin. Such an approach has demonstrated its accuracy in establishing the link between basin erosion and landscape change during long time scales (Edwards and Whittington, 2001).

This work, based on quantification of minerogenic phases of sediments by Fourier transform infrared (FTIR) spectroscopy provides information on:

1. the characterization of the present-day sedimentary dynamics in Lake Ossa (southwest Cameroon) using the modal

terrigenous mineral distribution in the superficial deposits and its relationship with the hydrological balance,

2. the terrigenous mineral content variations in the Late Holocene expressed as mineral fluxes, based on the analysis of core OW4 from Lake Ossa, considering these mineralogical variations along with the palynological and diatoms data (Reynaud-Farrera *et al.*, 1996; Nguetsop *et al.*, 1998), we are able to identify the probable climate-driven mechanisms involved in the observed environmental changes.

STUDY AREA

The study area is located in Cameroon (lat. 3°50′ N, long. 10° E) near the Gulf of Guinea (Fig. 1). It corresponds to the catchment basin (204 km^2) of lakes Ossa (37.6 km^2), Mévia (7.5 km^2), and Mwembé (2.8 km^2). This lacustrine complex is bounded by two sets of deep-seated faults, trending N40° E to N65° E and N150° to N170° E, and forms part of a tectonic unit of post-Eocene age located on the edge of the Douala basin (Elf-Serepca, 1987; Njiké Ngaha, 1984). The present-day water bodies were formed recently, probably after 18,000 cal yr B.P., after the silting up of the southern border of the catchment basin by alluvium from the Sanaga River.

The studied catchment basin is a low-lying plain (Fig. 2) made up of spherical hillocks separated by fairly steep-sided valleys. The mean height above sea level is about 60 m, with the highest point at 165 m on the eastern edge of the catchment (Wirrmann, 1992). The interfluves are covered by a network of near-perennial brooks that are more numerous in the northern part of the catchment (Fig. 2A). The higher ground is bordered by low-lying areas that are flooded by water sheets of variable extent and with depths of less than 8 m. These water sheets are at an elevation of 8 m above sea level and the lakes Mwembé, Ossa, and Mévia have a 3-km-long common outlet to the Sanaga River (Fig. 2). The total thickness of lacustrine sediment is unknown. For the period January 1993 to December 1996, our field observations show the rapid response of lake level to modern precipitation patterns. The highest lake levels occur with a short time delay after the rainiest month, and the lowest lake levels occur at the end of the dry season. With respect to the base level (8 m asl) the mean amplitude of oscillations in water depth is +4.5 m each year. The highest water stages are marked on some places along the shorelines by vegetationless sandy strands.

The catchment soils are derived from Tertiary sedimentary rocks. In the whole catchtment basin the soils are fairly homogeneous, and there is a sole rocky outcrop located at the northern border of the marshy area adajacent to Lake Mévia (Fig. 2B). The soils are represented by yellow leached ferralitic type soils associated with hydromorphic soils in the interfluves (Ségalen, 1994). They are sandy to sandy-argillaceous, consisting dominantly of quartz and subordinate kaolinite (the only clay mineral that is present), associated with variable but small amounts of gibbsite and goethite. Locally, traces of other primary minerals, such as feldspars, derived from the parent rock, are also observed (Ségalen, 1994).

The Lake Ossa region is located in the permanent Atlantic monsoonal domain. It has a seasonal equatorial climate (Suchel, 1988) characterized by a dry season of three months (December to February, with less than 50 mm monthly precipitation) followed by nine rainy months. A decrease in rainfall during June marks the "little dry season." Annual rainfall averaged 2947 mm at the S.A.F.A. CAM station (Société Africaine, Forêts et Agriculture, Cameroun) for the years 1952–1996 (Fig. 2B) and ranged between 2154 and 3770 mm. According to the year, the rainiest months correspond to August or September. The vegetation is a

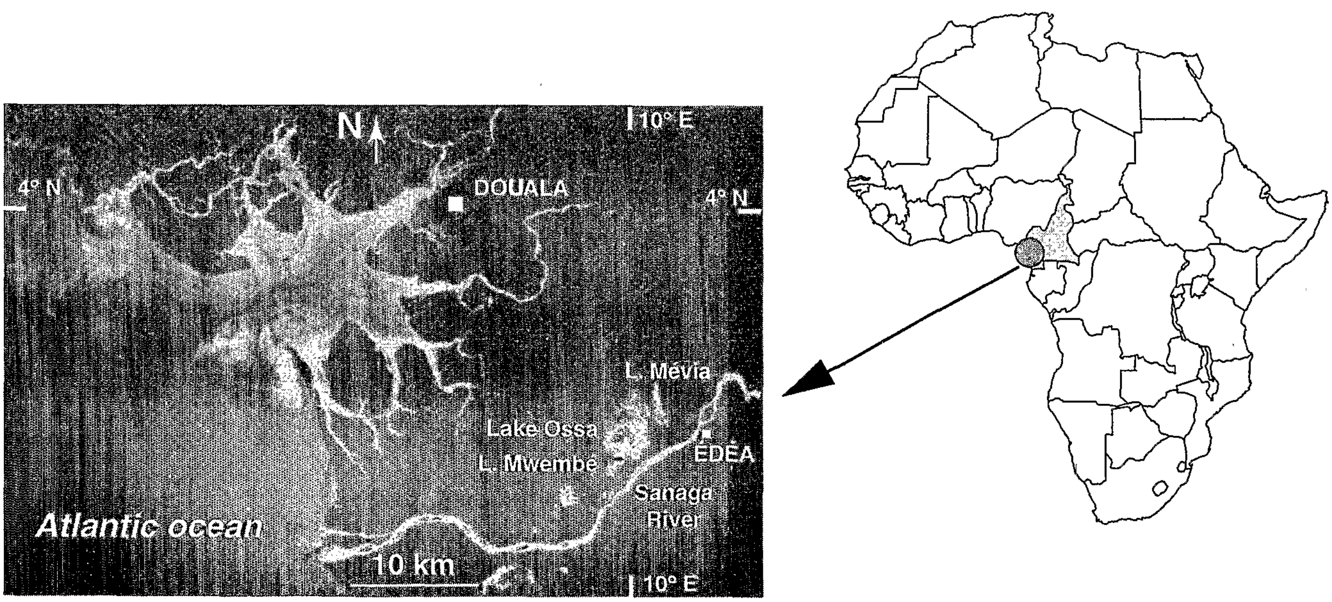

FIG. 1. Aerial view of the study area (combination of a Landsat photograph and a radar image).

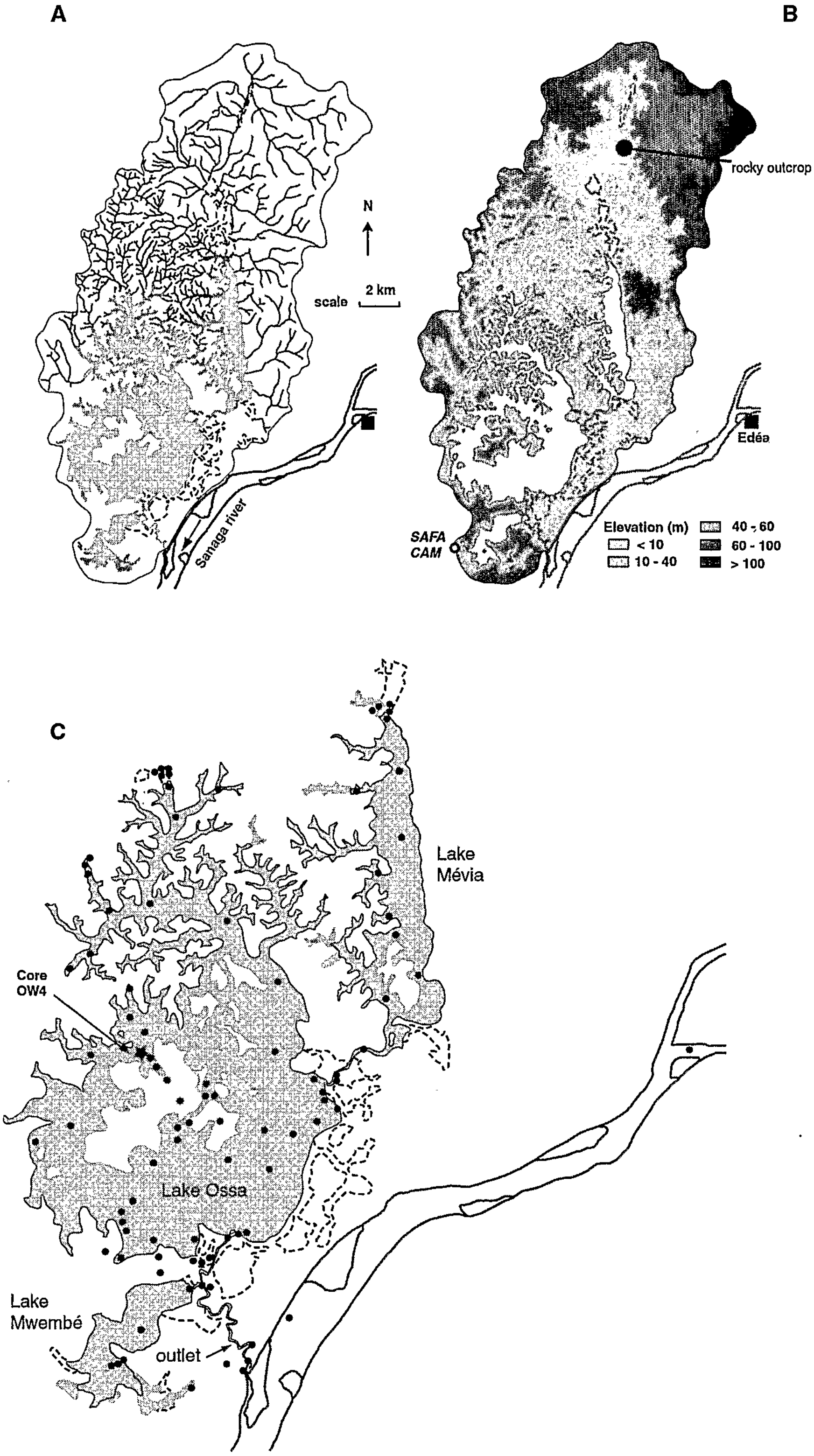

FIG. 2. Main characteristics of Lake Ossa catchment. (A) Hydrology (dashed lines represent permanent marshes); (B) topography; (C) localization of samples.

tropical lowland rainforest of the Guinean-Congolian type, defined by White (1986) as an ombrophilous evergreen Biafrean forest. Its principal characteristic is a high proportion of trees pertaining to the Caesalpiniaceae family (Letouzey, 1985). Since the beginning of the 20th century the forest has been replaced on the southwestern banks of Lake Ossa by commercial plantations of *Hevea* and oil palm (Anonymous, 1990). On the eastern parts of the catchment, recent human activities (food-producing cultivation, clear-cut logging) have also altered the rainforest cover. Former human settlement is poorly documented, especially for the Cameroonian Atlantic littoral area. So far, the only evidence of earlier human settlement in the Lake Ossa catchment is related to the Late Iron stage, which is dated at between 700 and 500 cal yr B.P. (Wirrmann and Élouga, 1998). On a local scale, human impact may have been significant from that time on, as the need of wood for iron reduction may have been conducive to land clearance on small forest areas.

SAMPLES AND METHODOLOGY

This work links present-day distribution of sediment types to the environmental conditions that produced the sediment. In a tropical forest environment, surface runoff remains weak outside of cleared areas, and detrital inputs do not originate from overland flow (Schwartz *et al.*, 2000) but rather from the scouring of river banks that provide the solid load according to the river discharge. Thus, the primary control on sediment supply is the volume of water flow such that the amount of particle transport into the basin depends on the rainfall intensity. Such a relationship between monsoon precipitation and the solid discharge load of rivers is evident throughout intertropical woodlands, and has been documented both in large catchments (Giresse and Barusseau, 1989; Orange *et al.*, 1995; Schneider *et al.*, 1997) and in smaller ones (Cook *et al.*, 1998). Due to the homogeneity of the soils from Lake Ossa catchment, the sole source of minerogenic inputs into the lake, the only cause of differentiation of sediment types is the energy level of the depositional environment. Two main lacustrine sediment types are recognized, corresponding to the preferential inner lake water path flow zones and to the sheltered areas, respectively. Hence, at a given location in the lake, variation of sediment types on long Holocene time scales can be related either to local conditions, e.g., changes in patterns of water movement through the lake, or to a regional climatic shift in rainfall. The proposed multiproxy approach gives clues to discriminate between these two causes.

Mineralogical Analysis

Quantification of the mineralogy of present-day deposits is derived from the analysis of 140 samples distributed over the whole basin (Fig. 2C). These samples represent superficial deposits that were collected in the water bodies, in some of the tributary inflowing brooks and from marshy sites or soils and spring-heads' exsurgences. The interpretation of the changes in sedimentation during the Late Holocene is based on the analysis of a 8-cm-diameter and 555-cm-long profile (OW4) taken by vibracore. This core (located at 3°48.3′ N, 10°0.6′ E) was retrieved during the dry season from 1.75-m water depth in a sheltered zone located to the northwest of the largest island in Lake Ossa (Fig. 2C). The whole core was subsampled continuously in cubic boxes of 6.67 cm^3. In addition, 36 samples—each of 1-cm depth—were taken for mineralogical studies, with a 5- to 20-cm sampling interval. The dry density of the sediment was obtained by weighing the cubes after drying for 8 days at 40°C.

Smear slides of bulk sediment from each sample were used to identify the different constituents and to estimate their relative abundance and particle size. Qualitative analysis was first carried out by XRD on some samples of bulk sediment and the clay-size fraction. Then, quantitative modal analyses of the main mineral constituents present in the sediment (quartz, kaolinite, gibbsite, orthoclase, and siderite) were obtained by FTIR spectroscopy for the entire set of samples, applying the analytical method developed by Bertaux *et al.* (1998). Mid IR spectra of the ground sediment in KBr pellets were measured and compared to spectra of pure mineral phases similar to the ones found in the sediments. Each spectrum represents the IR absorbance, which is linearly correlated to the composition and the mass of constituents in the KBr pellet. Spectra of the pure mineral phases are mathematically processed to determine the proportion of the mineral constituents from sediments. The good correlation between quantitative results from FTIR spectroscopy and chemical analyses has been presented and discussed elsewhere (Bertaux *et al.*, 1998). The FTIR results are expressed in weight percent of dry sediment, which allows a direct conversion into fluxes (see below). The results were then compared with the palynological and diatom data obtained on the same core (Reynaud-Farrera *et al.*, 1996; Nguetsop *et al.*, 1998).

Chronology

The dating of core OW4 was based on eight accelerator mass spectroscopy radiocarbon ages obtained on bulk organic matter (Table 1), excluding the macroflora remains represented by only three unidentified seed-cases (Fig. 4). The calibration of the conventional ^{14}C ages was carried out according to the

TABLE 1
Core OW4, ^{14}C Age Determination

Depth in core (cm)	Lab number	Age (^{14}C yr B.P.)	$\delta^{13}C$ (‰ PDB)	^{13}C adjusted age (yr B.P.)	Age range (cal yr 1σ)
6.8–9	Beta 73082	140 ± 60	−27.9	90 ± 60	20–260
62.7–64.9	Beta 86769	800 ± 50	−28.7	740 ± 50	655–689
122.9–125.1	Beta 73083	1970 ± 60	−29.8	1890 ± 60	1730–1880
174–175	UtC 3911		−32.3	2440 ± 40	2356–2705
243–245.2	Beta 73084	3430 ± 50	−31.0	3330 ± 50	3471–3626
358.8–360	Beta 73085	3980 ± 60	−30.9	3880 ± 60	4160–4410
523.6–525.8	Beta 73086	4650 ± 50	−29.4	4580 ± 50	5085–5317
548.3–550.5	Beta 73087	4850 ± 60	−29.9	4770 ± 60	5335–5590

Note. All the samples correspond to the disseminated organic matter separated from bulk sediment.

dendrochronological correction factors of Stuiver and Pearson (1993, MacCALIB 3.0.3c program) from $\delta^{13}C$ normalized ages without correction for the old carbon effect (we have no idea of its value in this area). The distribution of the calibrated dates and their relative 1-sigma ranges as a function of core depth were used to calculated an interpolated calibrated age for each analyzed sample, using a smoothing second-order polynomial (Edwards and Whittington, 2001), and the average sedimentary fluxes were determined for each mineral constituent by applying the following equation:

$$\begin{aligned} \text{sediment flux} &= \text{mineral abundance}\,(\%) \\ &\quad \times \text{sediment density}\,(\mathrm{g \cdot cm^{-3}}) \\ &\quad \times \text{sedimentation rate}\,(\mathrm{cm \cdot yr^{-1}}). \end{aligned}$$

These fluxes, expressed in $\mathrm{mg \cdot cm^{-2} \cdot yr^{-1}}$ are assumed to represent the input of each constituent independent of any dilution effect.

RESULTS AND DISCUSSION

Present-Day Mineral Distribution

Quartz, kaolinite, orthoclase, and gibbsite comprise the mineralogical fraction of the sediments and are associated with organic matter (mainly amorphous particles) and amorphous biogenic silica (mainly diatoms and few phytoliths) that form the remaining sediment fraction. The mean total carbon content in the sediments ($n = 67$ samples) is about 10%.

Kaolinite and quartz account for up to 74 and 94 weight% of the deposits, respectively, and are the main mineral constituents of the lacustrine sediments and soils, whether considered cumulatively or singly. They are associated with orthoclase (up to 22 weight%) and traces of gibbsite (up to 4.5 weight%).

Relatively high abundances of quartz (Fig. 3A) are encountered in the northern parts of lakes Ossa and Mévia, in particular near the shore and at the outlets of inflowing brooks, as well as at the outflows of these lakes and in the soil samples. The distribution of kaolinite is opposite that observed for quartz. Kaolinite is more abundant in the central parts of the water bodies (Fig. 3B) and is rare or even absent at the mouths of inflowing brooks and at lake outlets. Orthoclase is found only in very small proportions, accounting for less than 1% of the mode in 70% of the samples collected from Lake Ossa. However, orthoclase reaches its maximum abundance in the northern part of Lake Mévia, in the southeastern part of Lake Ossa, and at its outlet (Fig. 3C). Gibbsite is found in low amounts in all samples, but it is more abundant in sediments from Lake Mévia and from samples taken in the marsh located between lakes Ossa and Mwembé (Fig. 3D). The relative proportions of kaolinite versus those of quartz and orthoclase taken together, expressed as the ratio K/(Q + O), can be used to characterize different zones in the study area. Each of these zones corresponds to a specific particle transport pattern in relation to the water flow and/or runoff that prevailed in the sedimentation area. Each type of environment is characterized by a particular trend of mineralogical composition (Table 2). Two main groups of deposits (Fig. 3E) are differentiated by the values of their K/(Q + O) ratio: (1) sediments characterized by very low ratios (<1), corresponding to the soils and stream channels, and (2) sediments with higher ratios correlated with the inner lake area or the marshy environment. The marshes are differentiated from the inner lake areas by their lower K/(Q + O) ratios.

TABLE 2
Mean Mineralogical Composition (in Weight %) in Relation to Different Environment Types

Environment	Quartz	Orthoclase	Kaolinite	Gibbsite	K/(Q + O)
soils ($n = 9$)	57	0	30	0	0.52
exsurgences ($n = 3$)	39	0	27	0.2	0.69
river bottom ($n = 10$)	37	7	21	0.5	0.47
river outlet ($n = 8$)	70	6	7	0.1	0.09
inner L. Ossa ($n = 73$)	4	0.6	54	1.1	11.7
marsh ($n = 8$)	3	1.5	43	1.3	9.5

Quartz, kaolinite, and gibbsite are found in the present-day lacustrine sediments and are also the dominant phases making up the ferrallitic soil assemblages in the catchment (Ségalen, 1994). This shows that the catchment soils are the source of the detrital inputs into the lakes. The gibbsite distribution suggests that this mineral is a marker of zones immediately adjacent to the steepest slopes in the catchment. Steep relief facilitates more intense physical erosion of the soils, which results in greater mobility of minerals from the deeper parts of the soil profiles. In this way the proximity of steep slopes to the lake enhances the deposition of gibbsite in the lacustrine sediments. This interpretation is consistent with the absence of gibbsite in the superficial soils (Table 2). It also agrees with observations relative to similar rainforest soils from Amazonia showing that gibbsite does not occur at the top of the soil profiles but only at their base (Lucas *et al.*, 1993). Orthoclase is a primary mineral relic and is also found to be absent in the superficial soil samples (Table 2). Its origin may be related either to the deepest parts of the soil profiles or to the remobilization of preexisting fluvial sediments through lacustrine flooding. As the highest percentages of orthoclase are recorded in the northern part of Lake Mévia and in the part of Lake Ossa that receives waters from Lake Mévia, its parent rock could be the rocky outcrop (today a working stone-pit) located at the northern border of the marshy area adjacent to Lake Mévia.

This spatial distribution of terrigenous mineral in the sediments shows that the preferential feeding areas correspond to the northern banks of the water bodies (steepest slopes and highest topography, with a densely developed tributary network). The highest quartz and orthoclase amounts in the sediments reveal the zones where detrital input is currently active, and the medium to high percentage contents are seen to reveal the main paths of water flow in the lacustrine system. The importance of terrigenous mineral transport toward the lakes, as well

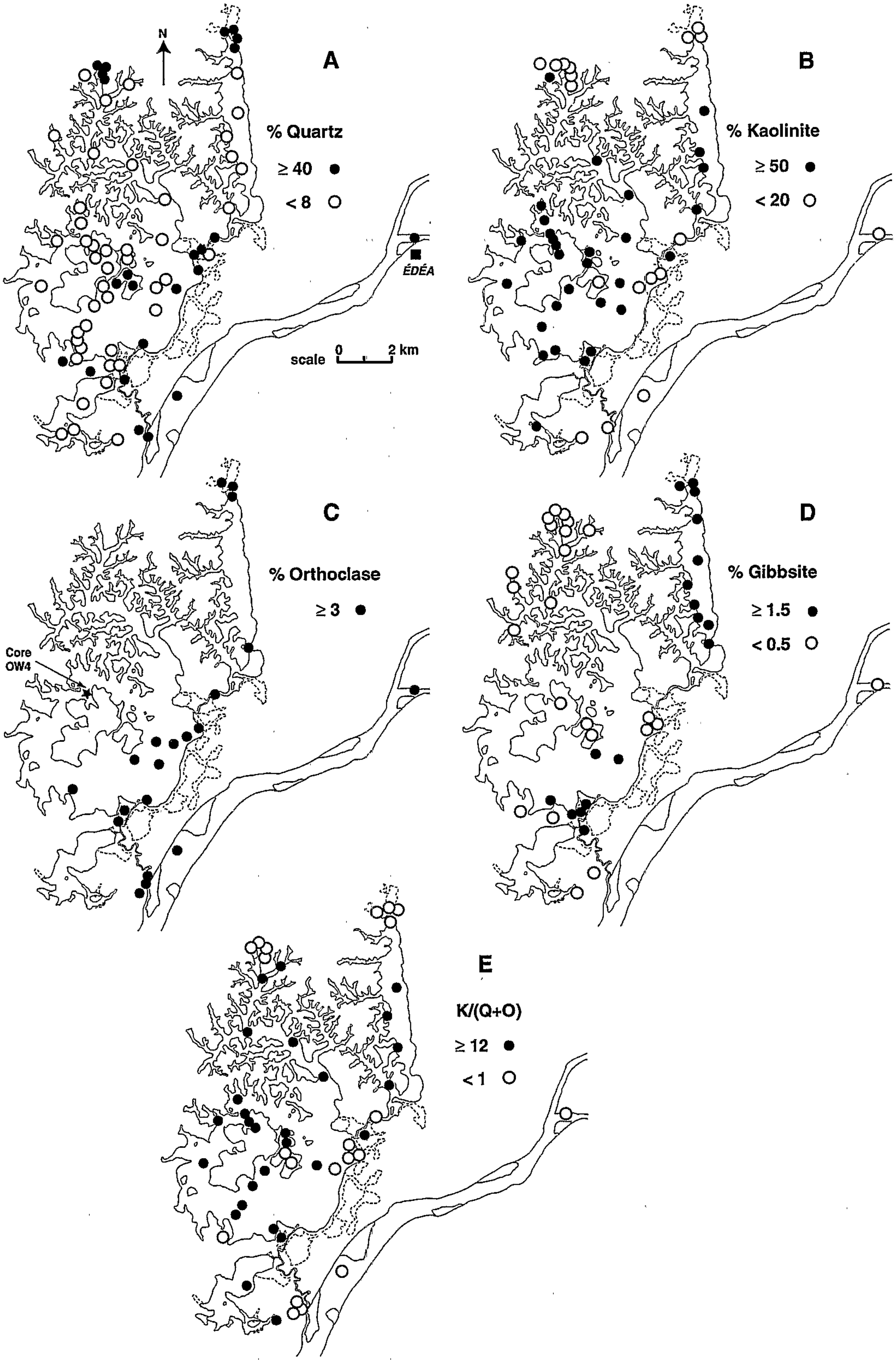

FIG. 3. Spatial distribution of mineral constituents in surface sediments, determined by FTIR spectrometry. Only the higher and/or lower range values are reported to facilitate the legibility of the maps.

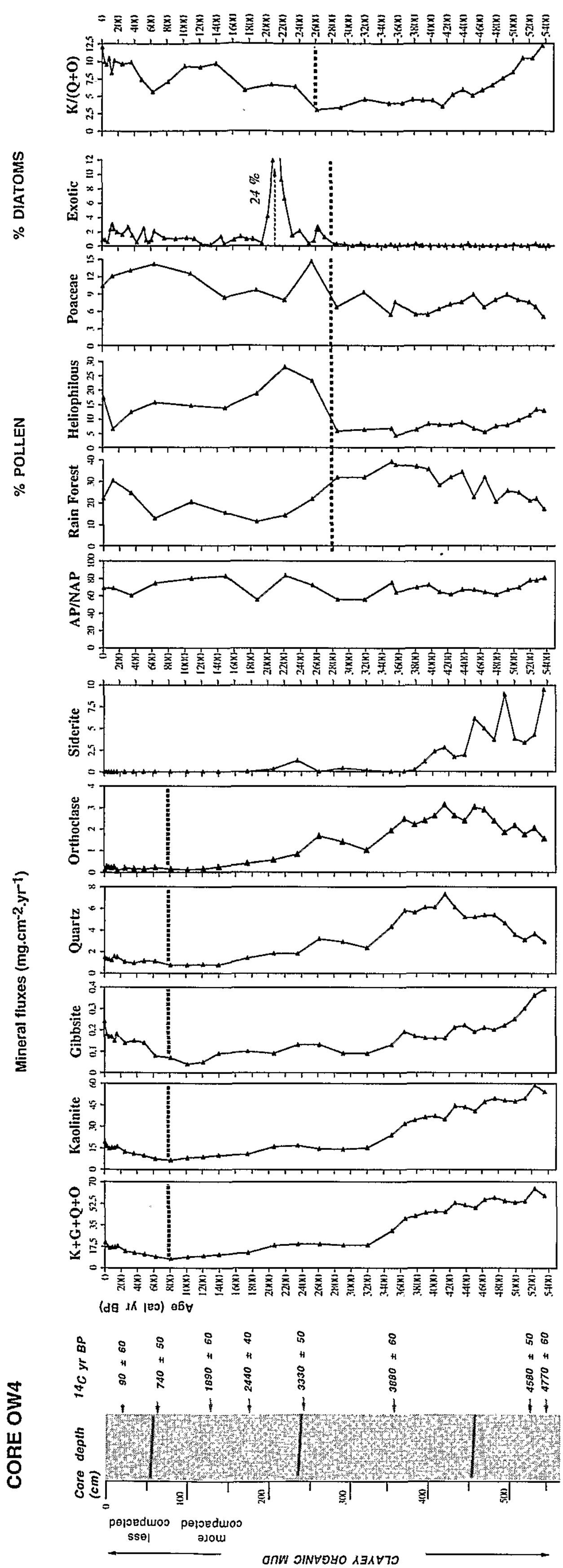

as within the water bodies themselves, depends on the intensity of water flow. Areas enriched in quartz and orthoclase are more or less extensive in relation to the movement of water masses within the lakes. In this way, the intensity of rainfall activity on the catchment basin causes change in sedimentary dynamics recorded across the studied area. The drainage basin of Lake Mévia, as strictly defined, currently plays an important part in the present-day dynamics of detrital supply within the setting of the lacustrine complex, even though it covers an area of only 41 km^2, i.e., only 20% of the whole catchment basin.

Upper Holocene Sedimentation

Core OW4 has a length of 555 cm and lacks any trace of laminations or bioturbation. It is composed of clayey organic-rich mud of greyish olive-green color (5Y2.5/2) and is more compact from 85 cm downward (Fig. 4). Distributed throughout the sediment column are some millimeter-scale clusters of vivianite particles, which are more abundant toward the base of the core, as well as three seed-cases. After calibration, the ^{14}C ages obtained show that the sediment record covers a period from 5500 cal yr B.P. to the present day. Their distribution as a function of depth indicates that there has been no interruption in sedimentation. The interpolated calibrated ages obtained for each analyzed sample show that the resolution between the samples ranges from 25 to 295 yr, with the average resolution being ca 150 yr. The age distribution versus core depth reveals three phases of accumulation: (1) from the base of the core (depth interval 540–541 cm) up to 240–241 cm, corresponding to interpolated cal yr B.P. of 5360 to 3495, where the sedimentation rate was relatively high; 2) up to 70–71 cm (810 cal yr B.P.), where the profile records a clear slowing down of sedimentation; (3) above 70 cm, where the sedimentation rate increased.

The mineral constituents are the same as those encountered in the present-day superficial sediments, except at the base of the core. Between 555 and 140 cm, siderite occurs as small prismatic crystals (20–25 μm by 5–10 μm). In freshwater lakes, early diagenetic siderite formation requires the coexistence of ferric iron (Fe^{3+}) and CO_2 produced by the bacterial degradation of organic matter in the water–sediment interface, leading to anoxic conditions. These conditions promote the reduction of ferric iron to ferrous iron (Fe^{2+}) to bond with CO_2 to form siderite (Berner, 1971). Ferric iron in the catchment was probably derived from the soils and supplied as detrital iron oxides in the sediment load. Thus if adequate ferric iron is supplied to a lake system, the presence of siderite signals diagenetic anoxic conditions.

FIG. 4. Lithology of core OW4 (the black lines indicate occurrence of seed-cases), mineral fluxes (mg · cm^{-2} · yr^{-1}), K/(Q + O) ratio fluctuations, pollen diagram (selection of main taxa after Reynaud-Farrera *et al.* (1996)), and wind-blown diatom abundance variations (after Nguetsop *et al.*, 1998) in core OW4 plotted versus cal yr BP.

That is why siderite in continental fresh lakes is most common in the deepest zone of the water bodies and embayments, which are least influenced by waves and currents (Baker *et al.*, 1995; Zhang Xiouzhu *et al.*, 1996). Hence the absence of siderite may suggest a lowering of mean lake level or/and insufficient supplies of ferric iron.

Kaolinite remains the major constituent throughout the core, with an abundance always higher than 57 weight%. Quartz, orthoclase and siderite represent less than 13, 7, and 10 weight% of the sediments, respectively, while gibbsite remains less than 1 weight%. The respective percentages of each mineral fraction are presented as fluxes ($mg \cdot cm^{-2} \cdot yr^{-1}$) versus cal yr B.P. (Fig. 4). From the base of the core until ca 800 cal yr B.P., detrital inputs generally decreased, and from that date onward they increased slightly but remained lower than those of the basal core section. Kaolinite and gibbsite share the same pattern of fluctuations, as do quartz and orthoclase, which are the only constituents to show increasing fluxes between 5400 and 4100 cal yr B.P. Siderite is absent from ca 2000 cal yr B.P. onward. At deeper levels, its fluxes show a high variability, with a general decreasing trend from the base of the core until 3800 cal yr B.P., and between 3800–2000 cal yr B.P. it is present only at very low amounts. Since high amounts of siderite are correlated with the highest observed values of the other detrital inputs, its presence must be primarily associated with high-level detrital supplies into the lake.

The fluctuations in the $K/(Q+O)$ ratio differentiate three main episodes (Fig. 4). The first one extends from 5400 to 4100 cal yr B.P. and is characterized by a steady decline of the ratios. Then, up to 2600 cal yr B.P., they vary slightly around the lowest values recorded for the whole core profile. From 2600 cal yr B.P. onward, they increase in two steps, interrupted by a lowering trend between 1000 and 600 cal yr B.P.. By analogy with the modern distribution of terrigenous mineral in the sediments (Table 1), these variations are interpreted in terms of water flow strength: The two basal episodes are characteristics of an initial stage of relativly strong water flow followed by a stage of lower water flow.

Throughout the duration of the sedimentary record, the persistence of a forest environment is demonstrated by the relative proportion of arboreal pollen (AP) to nonarboreal pollen (NAP), expressed as the ratio AP/NAP (Reynaud-Farrera *et al.*, 1996): It remains higher than 55%, although the vegetation records several changes in its floral associations (Fig. 4). Two main states of the vegetation cover are clearly identified, with the change between the two occuring between 2800 and 2600 cal yr B.P. Before 2800 cal yr B.P., the vegetation is characterized by relatively high and increasing percentages of rainforest taxa (Caesalpiniaceae + Sapotaceae + *Martretia*) and low percentages of heliophilous taxa (pioneer trees such as *Alchornea* and *Macaranga* genus) and Poaceae. After 2600 cal yr B.P., the vegetation associations show an abrupt change, marked by increasingly abundant heliophilous taxa and Poaceae, which is coeval with a lowering in the importance of rainforest taxa. The maximum degradation of the rainforest, recorded between ca 2500 and 1500 cal yr B.P., was followed by a progressive recovery, which was interrupted between 1000 and 600 cal yr B.P. As human activities have been identified mainly between 700 and 500 cal yr B.P. (Wirrmann and Élouga, 1998), the observed rainforest degradation from 1000 until 600 cal yr B.P. might be related to human settlement. Indeed the forest cover is more sensitive to anthropogenic perturbation at the onset of its recovery.

The lacustrine environmental changes are also documented by the diatom analysis (Nguetsop, 1997; Nguetsop *et al.*, 1998). The present-day diatom associations in the sediments sampled in the Sanaga River are characterized by the presence of *Acanthes lanceolata* associated with *Cymbella silesiaca, Gomphonema lingilatiforme, Navicula pupula pupula, N. cryptotenella, Aulacoseira italica, N. concinna, N. haimansii,* and *Stauroneis crucicula*, all species that are absent either in the superficial sediments from the lakes or in the core profile. This observation shows that water inflow from the Sanaga River into the lacustrine basin or changes in patterns of water movement between the lacustrine complex and the Sanaga River never occured during the last five millenia. Throughout the core, according to the diatom paleoflora associations, a relative stability of the lacustrine environment is observed. Nevertheless, two notable environmental modifications are recorded along time: (1) The lowest amounts of planktonic diatoms are observed between 3000–2600 and 2200–2000 cal yr B.P., suggesting that the lake reached its lowest level during those time periods, and (2) from 2800 cal yr B.P. (Fig. 4), the appearance of exotic diatoms such as *Aulacoseira granulata* var. *valida, A. granulata* var. *tubulosa* and *Stephanodiscus neoastrea* occured suddenly. These exotic diatoms, typical of large and deep lakes, comparable to those occuring in the Lake Chad sediments, correspond to wind-blown diatoms (Nguetsop *et al.*, 1998). Their presence in Lake Ossa sediments marks a major transition in the windiness and/or aridity, and the time 2200–2000 cal yr B.P. must have been particularly windy and/or arid.

The consideration of these mineralogical results and the biomarker data together enable a more precise interpretation of the temporal relationship between hydrological variations and vegetational changes recorded in the core profile. This set of data shows that the lower part of the Late Holocene was wetter than the two last millenia, with the shift to drier conditions occuring during the time interval 2800–2600 cal yr B.P. However, given the regular decrease in detrital fluxes since the beginning of the mid Holocene, a progressive trend to drier conditions is recorded earlier in the mineral data than in the vegetation.

PALEOCLIMATIC INTERPRETATION

Present-Day Climatic Pattern over Western Central Africa

The modern rainfall pattern is directly correlated with the atmospheric dynamics, governed in the lower atmosphere by the circulation of the northeastern and southeastern trade winds (or trades). These winds converge toward the Meteorological Equator (ME), which corresponds to the tropical low-pressure belt

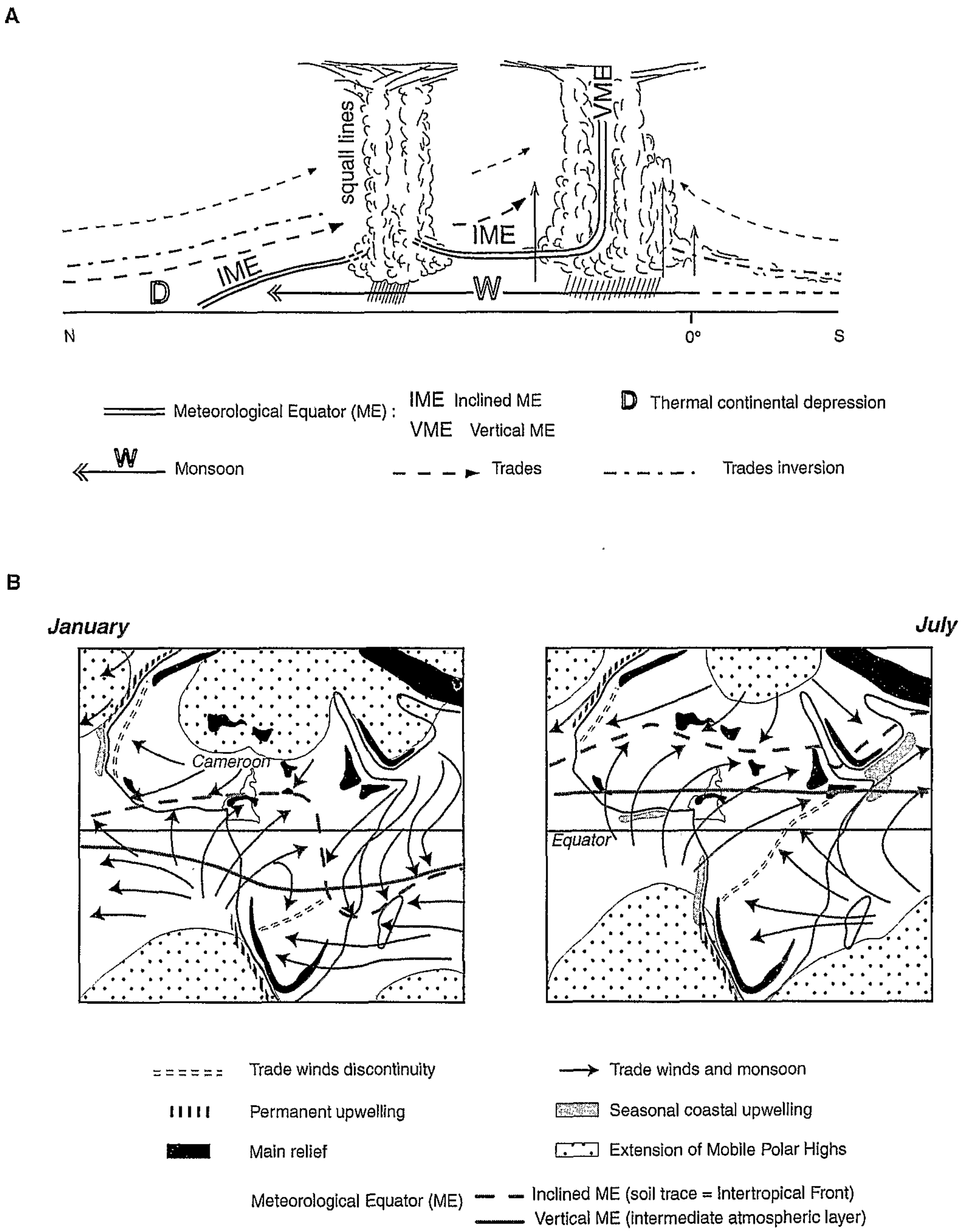

FIG. 5. Atmospheric general circulation pattern (adapted from Leroux, 1998). (A) Vertical structure of the Meteorological Equator over the continent during the boreal summer. (B) Present-day surface wind circulation over Africa during boreal summer and winter. See the text for explanations.

and which is also known as the Intertropical Convergence Zone over the ocean. The southeastern trades turn into southwestern Atlantic monsoon air flows as they cross the geographical equator, conveying humidity into the continent. The pluviometry is determined by the seasonal shift in the position of the ME (Fig. 5), in relation to the seasonal pattern of incident radiation, the atmospheric circulation being enhanced by the temperature contrast between land and ocean (Dupont *et al.*, 1998). Over the continent and at high altitudes (less than 500-hPa pressure) the ME presents a vertical structure (Fig. 5A), called Vertical ME (VME). It corresponds to the elongation of the oceanic structure, and fluctuates quite independently of the surface conditions between latitudes 10° and 12° South and North, during the boreal winter and the boreal summer, respectively (Leroux, 1998). In the lower atmospheric layers, the ME presents an inclined structure, forming a dipping plane that is the Inclined ME (IME), marking the boundary between the dry northeastern continental trades and the moist southwestern monsoon (Fig. 5A). Its seasonal migration is larger, being linked to the surface thermal conditions (between latitudes 23° S and 23° N). The VME corresponds to the maximum convective activity area (Lahuec, 1994) and, in turn, to continuous and abundant monsoon rains. By contrast, the IME induces random rainfall produced by squall lines and local storms of short duration. The different perturbations of the rainfall distribution in space and time are mainly due to (1) the availability of the Atlantic flow conveying precipitable water that controls the duration of the dry season and (2) permanent or seasonal inhibiting factors (Wauthy, 1983), such as subsidence of upper tropical air or cooling of lower air due to upwelling, which prevents water from falling in the upwelling neighboring continental areas. The first parameter is influenced by the sea-surface temperatures (Nicholson and Entekhabi, 1987; Janicot and Fontaine, 1997; Servain *et al.*, 1998), and the intensity of moisture exchange between ocean and the lower layers of air is reduced by cold oceanic waters.

Late Holocene

The changes in rainfall intensity with time are related to long-term monsoon circulation variations which are mainly driven by the 23,000-yr precessional cycle in low latitudes. The maximum boreal summer insolation in northern tropical latitudes induces maximum monsoonal inflow of moisture-laden air over Africa (Kutzbach and Street-Perrot, 1985; DeMenocal and Rind, 1993). From 11,000 yr onward, the orbital insolation has decreased regularly over the Northern Hemisphere at tropical latitudes (Berger and Loutre, 1991): At the present day, perihelion occurs during January, but 11,000 yr ago it occured during July, making Northern Hemisphere summers warmer than those of today. After a period of maximum insolation during the early Holocene, which lasted until ca 6000 yr B.P., the ongoing decrease of monsoonal intensity led to a general drier trend from the late Holocene onward, which marks the termination of the African Humid Period (DeMenocal *et al.*, 2000; Ritchie *et al.*, 1985). The progressive decrease of the fluxes observed in core OW4 after 5400 cal yr B.P. fits well with the regular decrease of boreal summer insolation over Africa and supports the interpretation of detrital mineral fluxes as proxies of mean rainfall intensity.

In this context of general rainfall decrease, the time interval 2800–2600 cal yr B.P. is a turning point that marks the onset of a dryness maximum. In the Gulf of Guinea area, previous studies have also documented the occurrence of such a climatic event. According to the hydrological sensitivity of the different studied regions, the paleoenvironmental changes will not present the same pattern. In the western Cameroonian region, drier conditions are recorded at Shum Laka cave between ca 3000 and 2000 yr B.P. (Moeyersons, 1997) and the vegetation cover around lakes Barombi Mbo, Mboandang, and Nyos record a rapid change characterized by an abrupt increase of Poaceae abundances from ca 2500 until ca 2000 yr B.P. (Giresse *et al.*, 1994; Richards, 1986; Zogning *et al.*, 1997). In Congo, drier conditions have also been documented at lakes Kitina and Sinnda between 2500 and ca 1100 cal yr B.P. These drier conditions, which are marked by the expansion of swampy and heliophilous arboreal taxa in the Kitina drainage basin and by the disappearance of the forest and the extension of open formations of savanna type in the Sinnda catchment (Elenga *et al.*, 1996; Vincens *et al.*, 1998, 1999), are coeval with a steady decline of mineral fluxes in both lakes (Bertaux *et al.*, 2000). The regional extension of this perturbation, and its synchronous onset, reflect an abrupt climatic change independent of human impact.

This change could have been caused by a modification in the temporal distribution of rains (i.e., the intensity of dry season) and/or oceanic cooler sea-surface temperatures, which in turn gave way to an increasing aridity in the Gulf of Guinea area by reducing the availability of moisture (Jansen *et al.*, 1996). During the boreal winter, when the IME is at its southernmost position, the dry northeastern continental trades (also called harmattan) blow off the northeastern African region into the Gulf of Guinea and give rise to the transport of aerosol (D'Almeida, 1986; Jankowiack and Tanré, 1992). The dusts originate mainly from the southern Saharan and Sahelian regions (Kalu, 1979), carrying windblown diatoms derived from the deflation of diatomaceous deposits in Saharan dry lake beds. From 2800 cal yr B.P. onward, the presence of exotic diatoms in the OW4 profile (Fig. 4) can be regarded as an indicator of harmattan penetration over the Lake Ossa catchment. Since the rapid degradation of the rainforest between 2600 and 2000 cal yr B.P. is coeval with the maximum abundances of exotic diatoms, the degradation of the forest is likely due to a change in the atmospheric circulation pattern of the trade wind system, which superimposed on the long-term monsoon changes.

One hypothesis that could explain the strengthening of the harmattan is a rapid atmospheric circulation mode (the glacial mode) presented recently by Leroux (1998). This author ascribes the strengthening of the trade winds to the anticyclonic movement in the tropics of Mobile Polar Highs (MPH), which are large lenses of cold air (Fig. 5B). In the lower atmospheric levels, these highs propagate from high latitudes toward the tropics in a southeasterly direction in the Northern Hemisphere and in a northeasterly direction in the Southern Hemisphere. Their strength depends on low initial temperatures in polar areas; the lower the temperature, the stronger will be the MPHs. The hypothesis of a rapid circulation mode from ca 2800–2600 cal yr B.P. in the Northern Hemisphere agrees with the evidence for a contemporaneous and abrupt climatic change to cooler and wetter conditions in the temperate and boreal zones of Europe, North America, and Japan at ca 800 cal B.C. (Brown *et al.*, 2000; Edwards and Whittington, 2001; van Geel *et al.*, 1996). Moreover, according to geochemical data obtained on the GISP2 Greenland ice core, each one of the recognized Holocene cold phases is characterized by an intensified polar atmospheric circulation in the North Atlantic area (O'Brien *et al.*, 1995). Thus, the environmental change recorded in the Lake Ossa catchment indicates a strong interrelationship between tropical and extratropical regions, documenting a strong, in-phase link between millenial-scale variations in high- and low-latitude climate during the middle Holocene. Van Geel *et al.* (1999) argue that the driving mechanism explaining this mid-Late Holocene climatic event might result from fluctuations in solar activity caused by changes in solar UV or solar wind and cosmic rays. This dry event is interrupted at ca 1000 cal yr B.P., despite the persistence of harmattan after that time, and this interruption is also recognized in Congo (Vincens *et al.*, 1998, 1999). These results suggest that this climatic event may also be sought in the coupled atmosphere–ocean surface system: A fall of sea-surface temperature (SST), leading to less convective activity in the lowlands caused by the formation of nonprecipitating stratiform clouds, may have played a role in combination with the strengthening of the harmattan. This scenario agrees with the increase of the precipitation/evaporation ratio at Lake Bambili (West Cameroon Highlands) observed between 2700 to ca 2000 cal yr B.P. (Stager and Anfang-Sutter, 1999), which is interpreted as a strengthening of stratiform cloud formation by the authors. The importance of the interrelations between sea-surface-temperature variability and the north–south shifts of the ME has been interpreted as a dominant forcing factor that accounts for climatic variability in the tropical Atlantic (Bigot *et al.*, 1997; Fontaine *et al.*, 1999; Kutzbach and Liu, 1997) and consequently moisture availability over the African continent.

CONCLUSION

This study shows that the distribution of mineralogical abundances with depth in Lake Ossa sediments records both the regional and local environmental conditions. The mineral composition of the sediment can be regarded as: (1) a proxy of mean rainfall intensity via the variations of mineral fluxes and (2) a proxy of water flow and/or runoff via the K/(Q + O) ratio.

A consideration of the mineralogical data and the biomarkers (pollen and diatoms) taken together enables a more precise interpretation of the paleoenvironmental changes recorded during the late Holocene. A general trend toward progressively drier conditions is recorded at least since 5400 cal yr B.P. This is linked to the regular long-term decrease of paleomonsoons related to the weakening of insolation in the tropical boreal summer. Within this general context, an abrupt climatic change toward a dryness maximum is superimposed onto the paleomonsoon variability. This event occured at 2800–2600 cal yr B.P. and lasted until ca 1000 cal yr B.P. and was related to a climatic pattern shift of global significance caused by a change in the lower atmospheric circulation. The change is characterized by the strengthening of northern trade winds, linked to a cold event in the northern high latitudes that is probably correlated with sea-surface-temperature variability in the eastern tropical Atlantic area.

ACKNOWLEDGMENTS

Financial and technical support was provided by IRD (Institut de Recherche pour le Développement, ex ORSTOM) through the research program PALÉOTROPIQUE (Paléoenvironnements Tropicaux et Variabilité Climatique, UR 55) and the IRD-CNRS research program ÉCOFIT (Écosystèmes et Paléoécosystèmes des Forêts Intertropicales).

REFERENCES

Anonymous. (1990). "Note de présentation de la S.A.F.A.-CAMEROUN." Rapport multigraphié, Dizangué, 11 pp.

Baker, J. C., Kassan, J., and Hamilton, P. J. (1995). Early diagenetic siderite as an indicator of depositional environment in the Triassic Rewan Group, southern Bowen Basin, eastern Australia. *Sedimentology* **43,** 77–88.

Berger, A., and Loutre, M. F. (1991). Insolation values for the climate of the last 10 millions years. *Quaternary Science Reviews* **10,** 297–317.

Berner, R. A. (1971). Diagenetic redox reactions in the system C-N-S-H-O. *In* "Principles of Chemical Sedimentology" (R. A. Berner, Ed.), pp. 115–137. Mc Graw-Hill, New York.

Bertaux, J., Frölich, F., and Ildefonse, P. (1998). Multicomponent analysis of FTIR spectra: Quantification of amorphous and crystallized mineral phases in synthetic and natural sediments. *Journal of Sedimentary Research* **68,** 440–447.

Bertaux, J., Schwartz, D., Vincens, A., Sifeddine, A., Elenga, H., Mansour, M., Mariotti, A., Fournier, M., Martin, L., Wirrmann, D., and Servant, M. (2000). Enregistrement de la phase sèche d'Afrique Centrale vers 3000 ans BP par la spectrométrie IR dans les lacs Sinnda et Kitina (Sud-Congo). *In* "Dynamique à long terme des écosystèmes forestiers intertropicaux" (M. Servant and S. Servant-Vildary, Eds.), pp. 43–49. IRD/UNESCO/MAB/CNRS, Paris.

Bigot, S., Maley, J., Laraque, A., Olivry, J. C., and Mélice, J. L. (1997). Le domaine forestier africain et ses marges: Les transitions majeures climatiques à l'époque actuelle et au cours des derniers millénaires. *In* "Les Temps de l'Environnement, Journées Pirevs" (CNRS, Ed.), pp. 255–262. CNRS, Toulouse.

Brown, S., Bierman, P., Lini, A., and Southon, J. (2000). 10 000 yr record of extreme hydrologic events. *Geology* **28,** 335–338.

Cook, P. J., Hatton, T. J., Pidsley, D., Herczeg, A. L., Held, A., O'Grady, A., and Eamus, C. (1998). Water balance of a tropical woodland ecosystem, Northern Australia: A combination of micro-meteorological, soil physical and groundwater chemical approaches. *Journal of Hydrology* **210,** 161–177.

D'Almeida, A. (1986). A model for Saharan dust transport. *Journal of Climate and Applied Meteorology* **24,** 903–916.

DeMenocal, P. B., and Rind, D. (1993). Sensitivity of Asian and African climate to variations in seasonal insolation, glacial ice cover, sea surface temperature and Asian topography. *Journal of Geophysical Research* **98(DA)**, 7265–7287.

DeMenocal, P. B., Ortiz, J., Guilderson, T., Adkins, J., Sarntheim, M., Baker, L., and Yarusinsky, M. (2000). Abrupt onset and termination of the African Humid Period: Rapid climate response to gradual insolation forcing. *Quaternary Science Reviews* **19,** 347–361.

Dupont, L. M., Marret, F., and Winn, K. (1998). Land–sea correlation by means of terrestrial and marine palynomorphs from the equatorial East Atlantic: Phasing of SE trade winds and the oceanic productivity. *Palaeogeography, Palaeoclimatology, Palaeoecology* **142,** 51–84.

Edwards, K., and Whittington, G. (2001). Lake sediments, erosion and landscape change during the Holocene in Britain and Ireland. *Catena* **42,** 143–173.

Elf-Serepca (1987). "Conclusions et recommandations du Groupe d'Interprétation Bassin de Douala." Rapport multigraphié 341-DE N°6/160, Douala, 30 pp.

Elenga, H., Schwartz, D., Vincens, A., Bertaux, J., de Namur, C., Martin, L., Wirrmann, D., and Servant, M. (1996). Diagramme pollinique Holocène du lac Kitina (Congo): mise en évidence de changements paléobotaniques et paléoclimatiques dans le massif forestier du Mayombe. *Comptes Rendus de l'Académie des Sciences, Paris, Série IIa* **323,** 403–410.

Fontaine, B., Janicot, S., and Roucou, P. (1999). Coupled ocean–atmosphere surface variability and its climate impacts in the tropical Atlantic region. *Climate Dynamics* **15,** 451–473.

Giresse, P., and Barusseau, J. P. (1989). Quaternary accumulation rates by hemipelagic and gravity current sedimentation on the Atlantic margin of

Africa: Control factors of advective and vertical flows. *Marine Geology* **89,** 279–297.

Giresse, P., Maley, J., and Brenac, P. (1994). Late Quaternary palaeoenvironments in the Lake Barombi Mbo (West Cameroon) deduced from pollen and carbon isotopes of organic matter. *Palaeogeography, Palaeoclimatology, Palaeoecology* **107,** 65–78.

Jankowiack, I., and Tanré, D. (1992). Les aérosols désertiques: Sources, transports, impacts déterminés par télédétection. *In* "Les climats subtropicaux et leur évolution: de l'observation spatiale à la modélisation" (CNES, Ed.), pp. 495–523. École d' Été de La Londe Les Maures CNES, Toulouse.

Janicot, S., and Fontaine, B. (1997). Évolution saisonnière des corrélations entre précipitations en Afrique guinéenne et températures de surface de la mer. *Comptes Rendus de l'Académie des Sciences, Paris, Série lla* **324,** 785–792.

Jansen, J. H. F., Ufkes, E., and Schneider, R. R. (1996). Late Quaternary movements of the Angola-Benguela front, SE Atlantic, and implications for advections in the Equatorial ocean. *In* "The South Atlantic: Present and Past Circulation" (G. Wefer *et al.*, Eds.), pp. 553–575. Springer-Verlag, Berlin-Heidelberg.

Kalu, A. E. (1979). The African dust plume: Its characteristics and propagation across West Africa in winter. *In* "Saharan Dust: Mobilization, Transport, Deposition" (C. Morales, Ed.), pp. 95–118. Wiley, Chichester.

Kutzbach, J. E., and Liu, Z. (1997). Response of the African monsoon to orbital forcing paramaters and feedbacks in the middle Holocene. *Science* **278,** 440–443.

Kutzbach, J. E., and Street-Perrot, F. A. (1985). Milankovitch forcing of fluctuations in the level of tropical lakes from 18 to 0 kyrs. *Nature* **317,** 130–134.

Lahuec, J. P. (1994). "Climatological" references: Interannual monthly averages. *In* "Satellite Monitoring of the Climate. Climatic-Monitoring Atlas: 1986–1994 (Africa and the Intertropical Atlantic)" (J. P. Lahuec and B. Guillot, Eds.), pp. 31–35. MÉTÉO-FRANCE-ORSTOM, Paris.

Leroux, M. (1998). "Dynamic Analysis of Weather and Climate." Wiley, London, 365 pp.

Letouzey, R. (1985). "Notice de la carte phytogéographique du Cameroun au 1/500 000." Institut de la Carte Internationale de la Végétation, Toulouse and IRA Yaoundé, 240 pp.

Lucas, Y., Luizão, F. J., Chauvel, A., Rouiller, J., and Nahon, D. (1993). The relation between biological activity of the rain forest and mineralogical composition of soils. *Science* **260,** 521–523.

Maley, J. (1991). The African rain forest vegetation and palaeoenvironments during Late Quaternary. *Climatic Changes* **19,** 79–98.

Maley, J. (1996). The African rain forest—Main characteristics of changes in vegetation and climate from the Upper Cretaceous to the Quaternary. *Proceedings of the Royal Society of Edinburgh* **104,** 31–73.

Moeyersons, J. (1997). Geomorphological processes and their palaeoenvironmental significance at the Shum Laka cave (Bamenda, western Cameroon). *Palaeogeography, Palaeoclimatology, Palaeoecology* **133,** 103–116.

Nguetsop, V. F. (1997). "Évolution des environnements de l'Ouest Cameroun depuis 6000 ans, d'après l'étude des diatomées actuelles et fossiles dans le lac Ossa. Implications paléoclimatiques." Unpublished thesis, Muséum National d'Histoire Naturelle de Paris, 278 pp.

Nguetsop, V. F., Servant, M., and Servant-Vildary, S. (1998). Paléolimnologie et paléoclimatologie de l'Ouest Cameroun au cours des 5000 dernières années, à partir de l'étude des diatomées du lac Ossa. *Comptes Rendus de l'Académie des Sciences, Paris, Série IIa* **327,** 39–45.

Nicholson, S. E., and Entekhabi, D. (1987). Rainfall variability in equatorial and southern Africa: Relationship with sea surface temperatures along the southwestern coast of Africa. *Journal of Climate and Applied Meteorology* **26,** 567–578.

Njiké Ngaha, P. R. (1984). "Contribution à l'étude géologique, stratigraphique et structurale de la bordure du bassin atlantique au Cameroun." Unpublished thesis, Université de Yaoundé, 131 pp.

O'Brien, S. R., Mayewski, P. A., Meeker, L. D., Meese, D. A., Twickler, M. S., and Whitlow, S. I. (1995). Complexity of Holocene climate as reconstructed from a Greenland ice core. *Science* **270,** 1962–1964.

Orange, D., Olivry, J. C., and Censier, C. (1995). Variations et bilans des flux de matières particulaires et dissoutes de l'Oubangui à Bangui (1987–1992). *In* "Grands bassins fluviaux périatlantiques: Congo, Niger, Amazone" (J. C. Olivry and J. Boulègue, Eds.), pp. 147–158. Collection Colloques et Séminaires, ORSTOM, Paris.

Pokras, E. W., and Mix, A. C. (1985). Eolian evidence for spatial variability of Late Quaternary climates in tropical Africa. *Quaternary Research* **24,** 137–149.

Reynaud-Farrera, I., Maley, J., and Wirrmann, D. (1996). Végétation et climat dans les forêts du Sud-ouest Cameroun depuis 4770 ans BP: analyse pollinique des sédiments du lac Ossa. *Comptes Rendus de l'Académie des Sciences, Paris, Série IIa* **323,** 749–755.

Richards, K. (1986). Preliminary results of pollen analysis of a 6,000 year core from Mboandong, a crater Lake in Cameroon. *In* "The Hull University Cameroon Expedition 1981–1982. Final Report" (R. G. E. Baker *et al.*, Eds.), Hull University Geography Department, Miscellaneous Series **30,** 14–28.

Richtie, J. C., Eyles, C. H., and Haynes, C. V. (1985). Sediment and pollen evidence for an early to mid-Holocene humid period in the eastern Sahara. *Nature* **330,** 645–647.

Schneider, R. R., Price, B., Müller, P. J., Ktoon, D., and Alexander, I. (1997). Monsoon related variations in Zaire (Congo) sediment load and influence of fluvial silicate supply on marine productivity in the East equatorial Atlantic during the last 200,000 years. *Paleoceanography* **12,** 463–481.

Schwartz, D., Vincens, A., Elenga, H., Alexandre, A., Bertaux, J., Servant, M., Servant, S., Nguetsop, F., Bonvallot, J., Guillet, B., Mariotti, A., de Namur, C., Reynaud-Farrera, I., Youta Happi, J., Delègue, M.-A., Fuhr, M., and ECOFIT members (2000). Réponse des végétations d'Afrique centrale atlantique (Congo, Cameroun) aux changements climatiques depuis l'Holocène moyen: pas de temps, variabilité spatiale. *In* "Les Temps de l'Environnement" (Presses Universitaires du Mirail and CNRS, Eds.), pp. 461–471. Université de Toulouse-Le Mirail, Toulouse.

Ségalen, P. (1994). Les sols ferralitiques et leur répartion géographique. *In* "Collection Études et Thèses," Vol. 1, pp. 40–89. ORSTOM, Paris.

Servain, J., Wainer, I., and Dessier, A. (1998). Évidence d'une liaison entre les deux principaux modes de variabilité climatique interannuelle de l'Atlantique tropical. *Comptes Rendus de l'Académie des Sciences, Paris, Série IIa* **327,** 1–8.

Stager, J. C., and Anfang-Sutter, R. (1999). Preliminary evidence of environmental changes at Lake Bambili (Cameroon, West Africa) since 24,0000 BP. *Journal of Paleolimnology* **22,** 319–330.

Street-Perrott, F. A., and Perrott, R. A. (1993). Holocene vegetation, lake levels and climate of Africa. *In* "Global Climates since the Last Glacial Maximum" (H. E. Wright Jr. *et al.*, Eds.), pp. 318–356. Univ. of Minneapolis Press, Minneapolis.

Stuiver, M., and Pearson, G. W. (1993). High precision bidecadal calibration of the radiocarbon time scale, AD 1950–500 BC and 2500–6000 BC. *Radiocarbon* **35,** 18–31.

Suchel, J. F. (1988). "Les climats du Cameroun." Unpublished thesis, Université de Bourgogne, 1177 pp.

Van Geel, B., Buurman, J., and Waterbolk, H. T. (1996). Archaeological and palaeoecological indications of an abrupt climate change in the Netherlands, and evidence for climatological teleconnections around 2650 BP. *Journal of Quaternary Science* **11,** 451–460.

Van Geel, B., Raspopov, O. M., Renssen, H., van der Plicht, J., Dergachev, V. A., and Meijer, H. A. J. (1999). The role of solar forcing upon climate change. *Quaternary Science Reviews* **18,** 331–338.

Vincens, A., Schwartz, D., Bertaux, J., Elenga, H., and de Namur, C. (1998). Late Holocene climatic changes in western equatorial Africa inferred from pollen from Lake Sinnda, Southern Congo. *Quaternary Research* **50,** 34–45.

Vincens, A., Schwartz, D., Elenga, H., Reynaud-Farrera, I., Alexandre, A., Bertaux, J., Mariotti, A., Martin, L., Meunier, J.-D., Nguetsop, F., Servant, M., Servant-Vildary, S., and Wirrmann, D. (1999). Forest response to climatic changes in Atlantic equatorial Africa during the last 4000 years BP and inheritance on the modern landscapes. *Journal of Biogeography* **26,** 879–885.

Wauthy, B. (1983). Introduction à la climatologie du Golfe de Guinée. *Océanographie Tropicale* **18,** 103–138.

White, F. (1986). "La végétation de l'Afrique. Mémoire accompagnant la carte de végétation de l'Afrique UNESCO/AETFAT/UNSO." Recherches sur les ressources naturelles, Vol. XX. ORSTOM and UNESCO, Paris, 384 pp.

Wirrmann, D. (1992). Le lac Ossa: une monographie préliminaire. *Revue de Géographie du Cameroun* **XI,** 26–38 (and map outside text).

Wirrmann, D., and Élouga, M. (1998). Discovery of an Iron Age site in Lake Ossa, Cameroonian Littoral Province. *Comptes Rendus de l'Académie des Sciences, Paris, Série IIa*, **323,** 139–146.

Zhang, X., Wang, Y., and Lei, H. (1996). Authigenic mineralogy, depositionnal environments and evolution of fault-bounded Lakes of the Yunnan plateau, south-western China. *Sedimentology* **43,** 367–380.

Zogning, A., Giresse, P., Maley, J., and Gadel, F. (1997). The Late Holocene palaeoenvironment in the Lake Njupi area, west Cameroon: Implications regarding the history of Lake Nyos. *Journal of African Earth Sciences* **24,** 285–300.